P-OFDM: Spectrally Efficient Unipolar OFDM*

H. Elgala and T.D.C. Little
Department of Electrical and Computer Engineering
Boston University, Boston, Massachusetts
{*helgala, tdcl*}*@bu.edu*

April 15, 2014

MCL Technical Report No. 04-15-2014

Abstract–A novel OFDM signal format, polar-OFDM (P-OFDM), is proposed. P-OFDM offers twice as much spectral efficiency as state-of-the-art real-value unipolar OFDM formats. Inherently, the high PAPR is reduced and the numerical evaluation of the BER performance under dynamic-range constraint of optical sources demonstrates superior results.

Keywords: Modulation, optical communications.

*In *Proc. Optical Fiber Communication Conference and Exposition (OFC)*, March 13, 2014, San Francisco, CA, 2014. This work is supported by the NSF under grant No. EEC-0812056. Any opinions, findings, and conclusions or recommendations expressed in this material are those of the author(s) and do not necessarily reflect the views of the National Science Foundation.

1 Introduction

The spread of bandwidth intensive services such as the on-demand high-definition television (HDTV) and cloud services urges the need to provide high-speed broadband access. The fiber-to-the-home (FTTH) technology brings optical fiber cabling to individual end users and is capable of providing such high-speed wired access [1]. However, to support up to 1Gbps per user, the migration to next generation PON (NGPON) technology is inevitable [2]. Similarly, to support 1Gbps indoor wireless access, light-emitting diode (LED) luminaries can be used to transmit data wirelessly based on the visible light communications (VLC) technology [3]. As for the modulation techniques, orthogonal frequency-division multiplexing (OFDM) is a strong candidate for both technologies to achieve robust gigabit links. OFDM offers high spectral efficiency, adaptation through bit-loading and power allocation per sub-carrier and simple frequency-domain equalization (FDE) [3]. High data rates are supported through parallel transmission of high-order multi-level quadrature amplitude modulation (M-QAM) symbols on orthogonal sub-carriers. In intensity modulation-direct detection (IM-DD) transmission using OFDM, the real-value baseband OFDM signal modulates the instantaneous power of the optical carrier that is directly detected using a photo detector. Recently, the performance using plastic optical fibers (POFs) is investigated [4].

OFDM signals are characterized by high peak-to-average power ratio (PAPR), thus suffer from non-linear distortions, mainly caused by the optical source [5]. To deal with this issue, we propose a novel unipolar version of OFDM, named P-OFDM, to offer twice the spectral efficiency compared to the conventional asymmetrically clipped OFDM (ACO-OFDM) [6] or the recently proposed versions [7, 8, 9]. Thus, for the same data rate, half the amount of bits per sub-carrier is required (low order M-QAM symbols). In addition, the PAPR is inherently reduced to avoid complexity and overhead of PAPR reduction techniques and to support high bit-error ratio (BER) performance under dynamic-range constraint of optical sources. Throughout the paper, based on laser diodes (LDs), the focus is on presenting the P-OFDM characteristics and performance compared to ACO-OFDM. It is worth pointing out that this work is also applicable for the VLC technology based on either LEDs or LDs.

2 The P-OFDM System

The main building blocks of the proposed P-OFDM system are illustrated in Fig. 1. The data symbols are input to the QAM Modulator and the output complex symbols are assigned by the Mapper only to sub-carriers with even-index in the inverse fast Fourier transform (IFFT) operation, *i.e.,* $X_{2m+1} = 0, m = 0, \cdots, N/2-1$ and no Hermitian symmetry. The output of the IFFT has a useful symmetry (half-wave even symmetry) where the complex samples in the period from 0 to $\frac{NT}{2}$ $(x^l(n))$ are repeated again from $\frac{NT}{2}$ to NT $(x^r(n))$, *i.e.,* $x^l(n) = x^r(n)$ where N is the IFFT-length and T is the sampling period. This OFDM symbol is mathematically described as follows:

$$x_{n+N/2} = \frac{1}{N}\sum_{m=0}^{N/2-1} X_{2m}\exp^{\left(j\frac{2\pi}{N}(n+N/2)2m\right)} = \frac{1}{N}\sum_{m=0}^{N/2-1} X_{2m}\exp^{\left(j\frac{2\pi}{N/2}nm\right)}\exp^{j2m\pi} = x_n \qquad (1)$$

where, $x_n, n = 0, \cdots, N-1$ are the N time-domain output samples and the values $X_k, k = 0, \cdots, N-1$ are the N frequency-domain input symbols.

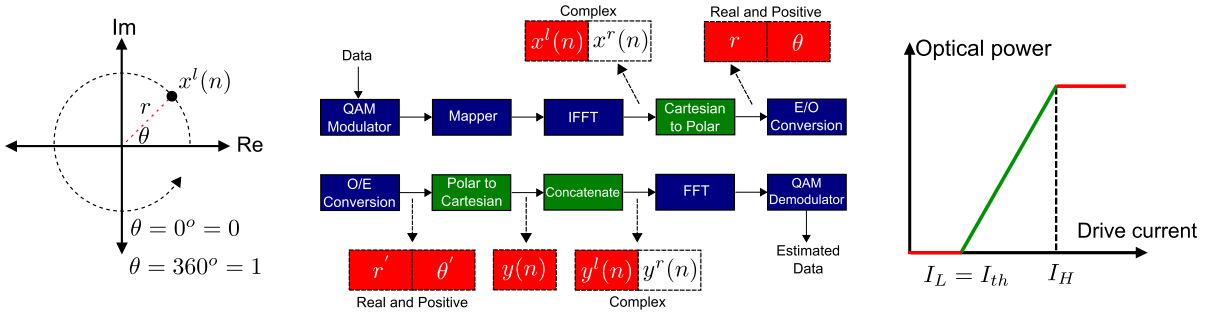

Figure 1: The main operations of the proposed P-OFDM system. Assuming I_H to correspond to the maximum drive current and I_L corresponds to the minimum drive current, the LD dynamic-range can be denoted by $I_H - I_L$ where I_{th} is the LD threshold current.

Thus only half the time is required to transmit this complex-value OFDM symbol. This situation offers the possibility of transforming the complex samples based on the Cartesian coordinate system to polar coordinate system using the Cartesian to Polar operation where the amplitudes of the different samples (r) are transmitted on the first half-period of the OFDM symbol while the phases of the different samples (θ) are transmitted on the second half-period of the OFDM symbol. After the photo detector, the received samples representing the amplitudes of the transmitted samples ($r^{'}$) and the phases of the transmitted samples ($\theta^{'}$) are used at the input of the the Polar to Cartesian operation to represent the transmitted complex samples again in the Cartesian coordinate system. The generated signal $y(n)$ is vertically concatenated with itself as illustrated in Fig. 1, *i.e.,* $y^l(n) = y^r(n)$. Finally, an FFT operation is applied to generate complex symbols and the QAM Demodulator operation is used to estimate the transmitted data symbols.

3 Key Parameters for Comparison

Spectral Efficiency and Complexity Compared to conventional OFDM used in RF (complex signals), the spectral efficiency of ACO-OFDM is one fourth, *i.e.,* $\frac{1}{4}\log_2 M$, as a result of limiting the data transmission on odd sub-carriers and due to the Hermitian symmetry. On the other hand, P-OFDM uses only even sub-carriers for data transmission, however Hermitian symmetry is not needed. Hence, P-OFDM offers twice as much spectral efficiency , *i.e.,* $\frac{1}{2}\log_2 M$. Based on Fig. 1, it can be concluded that the complexity of both P-OFDM and ACO-OFDM is almost the same, *i.e.,* excluding the conversion between the coordinate systems. Efficient conversion as well as polar Fourier transform are studied in [10, 11]

Transmitted Energy, SNR and BER In ACO-OFDM, the transmitted energy on the time samples is allocated to odd sub-carriers. On the other hand, in P-OFDM, the transmitted energy is allocated to even sub-carriers and spread across two parts: samples representing r and samples representing θ. In this paper, we present two approaches to allocate energy to samples of r and θ. The first approach, "P1-OFDM," a scaling factor m is directly applied to set the average power per OFDM symbol, however in the second approach, "P2-OFDM," a balanced energy spread "power balance approach" is ensured before applying m. At the receiver, this spread energy is recombined during the regeneration of the complex OFDM samples. The BER performance is directly related to the effective signal-to-noise ratio (SNR) that is equal to a conventionally defined SNR, *i.e.,* the ratio

between signal and noise powers, multiplied by a factor (less than 1) that is related to the clipping level [12].

Clipping Ratio The dynamic-range of the OFDM signal is constrained by the linear dynamic-range of the LD. For both ACO-OFDM and P-OFDM, clipping of lower signal peaks is avoided and no DC bias current is required, *i.e.,* $I_{DC} = I_{th}$. However, the upper peaks are limited in the form of clipping to achieve a lower effective PAPR. Thus the maximum sample amplitude of the clipped signal is assumed to be smaller or equal to dynamic-range. As long as the induced clipping distortion is comparable to the additive noise, system performance could be maintained. To investigate the dependance of the BER on the dynamic-range, the clipping ratio is defined in dB as $10\log_{10}\frac{\text{dynamic-range}}{\text{average power per OFDM symbol}}$.

4 Results

Monte-carlo simulations are conducted to compare the PAPR of P-OFDM with that of ACO-OFDM and to investigate the influence of M. The average power per symbol for both schemes is set to 15dBm, $I_H = 1A$ and $I_L = I_{th} = I_{DC} = 0A$. Modulating signal current values above 1A are clipped. Figures 2 shows the time samples of P-OFDM symbols using 3-bits, 4-bits and 5-bits per sub-carrier. It is clearly noticed that independent on the modulation order, the envelope of the θ samples is limited to 1 which corresponds to $\theta = 360^o$. Higher peaks for r samples are obtained at high order constellations. Figure 3 depicts the CDF plots of the PAPR for P1-OFDM and ACO-OFDM. Indeed, P1-OFDM has low PAPR as compared with ACO-OFDM for the same number of sub-carriers. In P1-OFDM, the PAPR is lower for high order constellations explained by the higher peaks for r samples at limited peaks of θ samples.

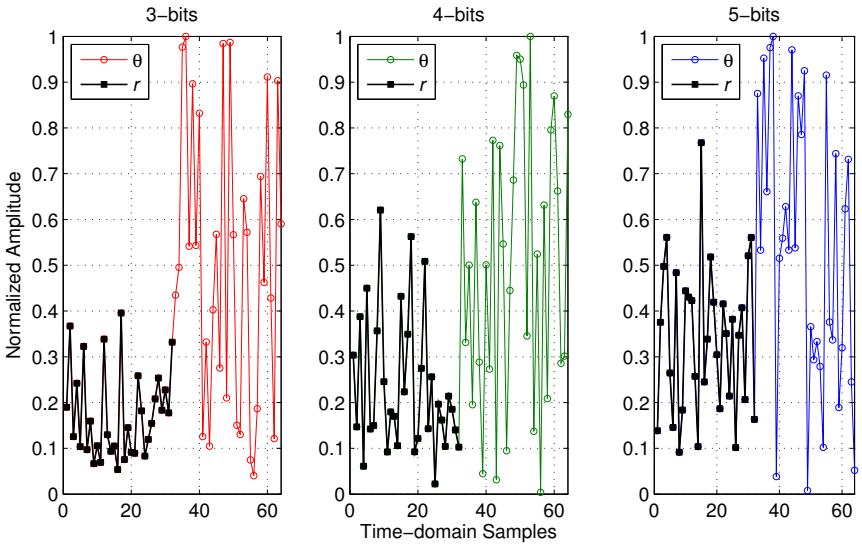

Figure 2: P1-OFDM symbols at different QAM constellations

The influence of the dynamic-range on BER curves is also investigated. Additive white Gaussian noise (AWGN) of -15dBm and perfect synchronization between the transmitter and the receiver are assumed. It is clearly confirmed that at the same data rate, P-OFDM offers superior BER

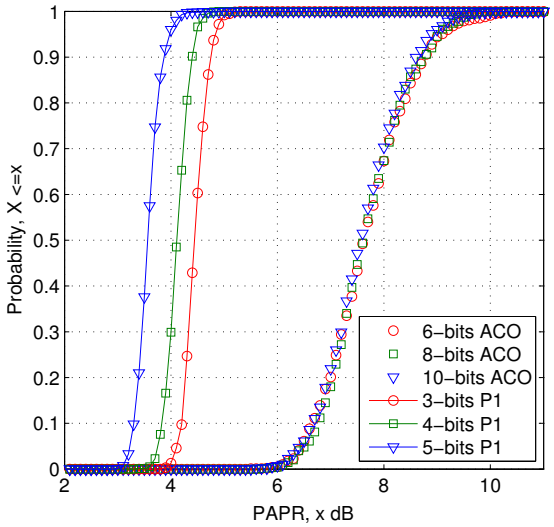

Figure 3: CDF plots of PAPR for $N = 64$ and different bits per sub-carrier.

performance for clipping ratio as low as 2dB (Fig. 4). For ACO-OFDM using 10-bits per sub-carrier, the BER floor is above the forward error correction (FEC) limit. For ACO-OFDM and a target BER of 10^{-3}, clipping ratios below 12dB are not sufficient even at 6-bits per sub-carrier. For P1-OFDM, a clipping ratio of 6dB is sufficient to achieve BER of 10^{-3} for 5-bits per sub-carrier, *i.e.,* corresponds to 10-bits using ACO-OFDM. Finally, using P2-OFDM, BER of 10^{-3} for 5-bits per sub-carrier is achieved at 4dB clipping ratio. A clipping ratio of 2dB supports BER below 10^{-3} for 4-bits and 3-bits per sub-carrier.

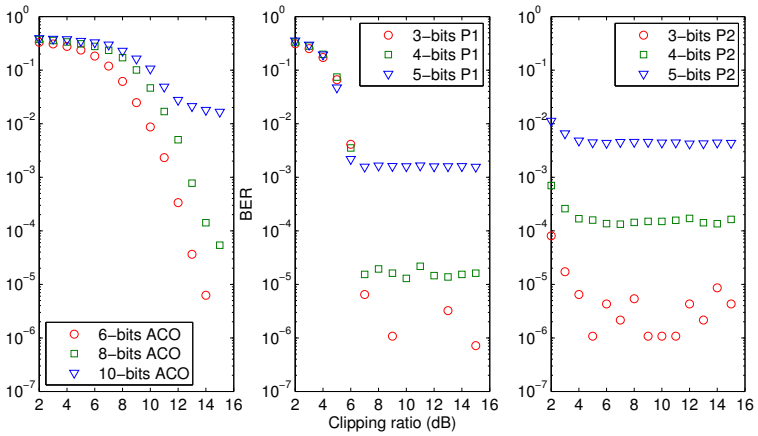

Figure 4: The BER vs. clipping ratio for ACO-OFDM, P1-OFDM and P2-OFDM.

5 Conclusion

The proposed spectrally efficient P-OFDM is analyzed and compared to the well-known ACO-OFDM in the context of IM-DD transmission. A BER lower than FEC limit is maintained while maximizing data rate even under a narrow LD dynamic-range. In addition, using a power balance

approach is shown to bring a significant BER performance even under narrower LD dynamic-range as low as 2dB clipping ratio.

6 References

[1] C. Lin, *Broadband Optical Access, FTTH, and Home Networks–the Broadband Future* (Wiley Online Library, 2006).

[2] E. Skaljo, M. Hodzic, I. Bektas, *ICUMT*, pp. 1–4 (IEEE, 2009).

[3] R. Mesleh, H. Elgala, H. Haas, *Journal of Optical Communications and Networking* **3**, 8, pp. 620–628 (IEEE/OSA, 2011).

[4] H. Yang, *et al.*, *OFC*, pp. 1–3 (OSA, 2009).

[5] R. Lin, *ACP*, Proc. of SPIE **8309**, paper 83091C (OSA, 2011).

[6] J. Armstrong, B. J. Schmidt, *Communications Letters* **12**, 5, pp. 343–345 (IEEE, 2008).

[7] N. Fernando, Y. Hong, E. Viterbo, *ITW*, pp. 5–9 (IEEE, 2011).

[8] A. Nuwanpriya, A. Grant, S.-W. Ho, L. Luo, *GC Wkshps*, pp. 1219–1223 (IEEE, 2012).

[9] D. Tsonev, S. Sinanovic, H. Haas, *VTC-Spring*, pp. 1–5 (IEEE, 2012).

[10] A. Averbuch, *et al.*, *Journal of Applied and Computational Harmonic Analysis* **21**, 2, pp. 145–167 (Elsevier, 2006).

[11] A. V. Agrawal, R. Mehra, *International Journal of Computer Applications* **64**, 20, pp. 31–37 (FCS, 2013).

[12] E. Vanin, *Optics Express* **19**, 5, pp. 4280–4293 (OSA, 2011).